PROCEEDINGS, 47th Workshop on Geothermal Reservoir Engineering
Stanford University, Stanford, California, February 7-9, 2022
SGP-TR-223

Nonlinear Finite Volume Discretization of Subsurface Flow and Mechanics Problem

Sree Rama Teja Tripuraneni [a,b], Aleks Novikov [b] and Denis Voskov [a,b]

[a]Dept. of Energy Resources Engineering, 367 Panama St., Stanford University, Stanford, CA, USA, 94305

[b]Faculty of Civil Engineering and Geosciences, Delft University of Technology, the Netherlands

teja1337@stanford.edu, a.novikov@tudelft.nl, d.v.voskov@tudelft.nl

Keywords: Finite volume method, Anisotropic linear elasticity, Anisotropic diffusion equation, Nonlinear discretization

ABSTRACT

Energy transition extends the range of geological settings and physical processes to be considered in subsurface reservoir modeling. Numerous applications consider essentially anisotropic reservoirs or require advanced gridding that cannot be resolved consistently by conventionally used Two Point Flux Approximation (TPFA). The presence of anisotropy and heterogeneity can occur in both permeability (porous media) and stiffness tensor (linear elasticity). Just like any subsurface formation, geothermal reservoirs can have fluvial channels, sand lenses, and spatial heterogeneity in permeability which will not give an accurate solution on non-K-orthogonal grids. A Finite Volume (FV) framework forms the basis for this project due to the local mass conservation property while solving the flow problem. When there are full tensor material properties, multipoint methods provide a good approximation of flux across interfaces. But these methods are known to be non-monotone which can introduce new types of numerical errors. So, we present a Nonlinear Two Point Flux Approximation (NTPFA) based on gradient reconstruction and homogenization function, and a Nonlinear Two Point Stress Approximation (NTPSA) where the linear elasticity equation is solved in FV framework using the nonlinear discretization technique instead of a multipoint approach. Currently, we treat both the models independently but the main idea of this kind of approximation is to integrate flow and mechanics in a unified nonlinear framework with minimal degrees of freedom, and we can derive the coupled equation for a poro-mechanical simulation. Reducing monotonicity in our primary variables can improve the accuracy of the traction component at the interface which is especially useful when we model displacement along the fault.

1. INTRODUCTION

The Finite Volume Method (FVM) provides a convenient framework in various engineering applications where advection, diffusion, and other types of physics drive nature [1]. The conservation laws involved within the domain are represented by a partial differential equation (PDE) which are approximated by the FVM to obtain the solution of an unknown variable for any point in space and time. The local mass conservation is an intrinsic property in FVM which makes it an ideal framework in the field of fluid mechanics.

Especially when we investigate deep geothermal simulation, the grids we have are often highly distorted because of the presence of impermeable zones, fractures, faults, or all together. These features not only complicate the geological model but also bring additional sensitivity. This sensitivity is related to the dynamic response of the reservoir to any perturbations in the geology. From a mathematical point of view, we can attribute these features to a heterogeneous permeability tensor which characterizes how easy fluid flows in porous media. Due to the presence of this heterogeneous and anisotropic permeability tensor, the conventional TPFA will not be a representative approximation of flux and gives up convergence. To tackle this problem, there have been numerous theories and developments, which help us conceptually understand how fluid flow is controlled by these complexities.

It started with the development of Multi-Point flux approximation (MPFA) schemes [2], [3], [4] and [5] where we utilize more than two cells for approximating flux across the interface between control volumes. The MPFA method generally gives an accurate approximation of flux across the interface where all or most cells surrounding the interface are considered. However, in many cases, MPFA methods are known to be conditionally monotone according to [6] and violate the discrete maximum principle (DMP) in extreme cases. This violation often takes the form of spurious oscillations in the numerical solution across the grid. There has been extensive research associated with how we can minimize these oscillations and make the MPFA discretization more robust.

To tackle this problem, a nonlinear formulation of the discrete flux equation was developed by [7] and [8] and then modified by various researches [9], [10], [11], [12], [13] and [14]. In this formulation, the linear elliptical equation is transformed to a nonlinear form such that the scheme becomes monotone. The idea of nonlinear Finite Volume (FV) approaches is that the flux approximations should have non-negative coefficients in front of unknowns which is pressure in our case. Specifically, in this paper, the Nonlinear Two Point Flux Approximation (NTPFA) we will follow is positivity preserving but does not satisfy the DMP condition.

Now after the MPFA procedure gained attention because of its ability to handle anisotropic discontinuous full permeability tensor, there have been attempts to formulate a similar type of Finite volume framework for linear elasticity problem in [15], [16], [17] and [18]. Although the research in the field of simulation of momentum equations by Finite Elements (FE) is more mature, the advantage of using an FV framework in mechanics is the ability to resolve coupled poro-mechanical problems by a unified FV framework. The local conservation guaranteed in the FV framework makes it more feasible to shift mechanics to FV rather than flow to FE.

This brings us to the main motivation behind this project. We will first develop NTPFA for multiphase flow problems in subsurface porous media with fracture network. Then we will also extend our method to mechanics by introducing Nonlinear Two Point Stress Approximation (NTPSA), which is a new discretization technique in FV mechanics. Next we analyze the traction profile along a fracture plane in the domain. The method is implemented in the DARTS platform, which is an open-source general-purpose simulation platform [19]. DARTS has been successfully applied to various energy transition applications including geothermal energy [20] and poro-mechanical simulations [21].

2. PROBLEM FORMULATION

The procedure followed in the flow problem is taken from both [22] and [12]. We will first discuss the governing equations for both flow and mechanics.

2.1 Multiphase Flow

We consider a two-phase two-component flow which assumes immiscible phases (each phase does not dissolve into one another). Water flooding into oil reservoir or high enthalpy geothermal systems can be modelled using these equations. Although for geothermal we also need to consider energy balance equation where we should account for EoS of water [20].

$$\frac{\partial(\boldsymbol{\phi}\boldsymbol{\rho}_{\mathfrak{a}}\boldsymbol{s}_{\mathfrak{a}})}{\partial \boldsymbol{t}} + \boldsymbol{\nabla}\cdot(\boldsymbol{\rho}_{\mathfrak{a}}\boldsymbol{v}_{\mathfrak{a}}) = \boldsymbol{f}_{\mathfrak{a}} \quad \text{in} \quad \boldsymbol{\Omega}, \tag{Eq-1}$$

$$\alpha\, p_{\mathfrak{a}} + \beta\, \mathbf{n}\cdot\boldsymbol{v}_{\mathfrak{a}} = \gamma \quad in \quad \partial\Omega, \tag{Eq-2}$$

$$\boldsymbol{v}_{\mathfrak{a}} = -\frac{k_{r\mathfrak{a}}\mathbb{K}}{\mu_{\mathfrak{a}}}\nabla p, \quad \mathfrak{a} = w \; or \; o, \tag{Eq-3}$$

where Ω is represents our domain, $\partial\Omega$ is the boundary, $\mathfrak{a} = \{w, o\}$ is the phase in our system, $s_{\mathfrak{a}}$ is the saturation, $\rho_{\mathfrak{a}}$ is phase density, $\boldsymbol{v}_{\mathfrak{a}}$ is Darcy velocity, $k_{r\mathfrak{a}}$ is relative phase permeability, $\mathbb{K}$ is permeability tensor and $\mu_{\mathfrak{a}}$ is viscosity of that phase. The source/sink is represented by $f_{\mathfrak{a}}$ and p is pore pressure. Different phases can have different pressures if we consider capillarity and gravity, but for the sake of simplicity we will not be including those terms. A general boundary condition is also considered in Eq-2, where values of α, β and γ can be varied and $\mathbf{n}$ is the normal vector of our interface/boundary face. In a simple case $\alpha = 0$, represents Neumann and $\beta = 0$, represents Dirichlet. We also consider compressible system where both phase density $\rho_{\mathfrak{a}}$ and porosity ϕ are functions of pressure.

2.2 Linear Elasticity

In this section we consider equations and physics involved in the mechanics problem. We assume the material is elastic, which represents the mechanical properties of unsaturated subsurface formations. We do not couple it with the fluid flow. The momentum balance equation looks as follows:

$$-\nabla\cdot\boldsymbol{\sigma} = \mathbf{f} \quad in \quad \Omega, \tag{Eq-4}$$

$$\alpha\mathbf{u_b} + \beta\boldsymbol{P}(\boldsymbol{\sigma}\cdot\mathbf{n}) = \mathbf{r} \quad in \quad \partial\Omega, \tag{Eq-5}$$

here $\boldsymbol{\sigma}$ is the stress tensor which is a 3x3 matrix, $\mathbf{f}$ is analogous to source/sink term in equation Eq-1 which corresponds to volumetric force vector 3x1, α and β values are similar to values used in equation Eq-2 , $\mathbf{u_b}$ is the displacement at the boundary interface, $\boldsymbol{P}$ is a 3x3 projection operator and $\mathbf{r}$ is similar to γ in equation Eq-2. We also need a stress-strain relationship which has the same purpose as equation Eq-3, so we consider Hooke's law in a continuous elastic medium as:

$$\boldsymbol{\sigma} = \mathbb{C} : \boldsymbol{\varepsilon} = \mathbb{C} : \frac{\nabla\boldsymbol{u} + \nabla\boldsymbol{u}^T}{2}, \tag{Eq-6}$$

here, the first part of equation Eq-6 is represented in tensorial form with $\mathbb{C}$ being 4th order material stiffness tensor, $\boldsymbol{\varepsilon}$ is the strain tensor. This equation can be rearranged in the format represented in second part of Eq-6 where $\nabla\boldsymbol{u}$ is the gradient of displacement (also 3x3 tensor). The roller boundary condition is also considered which is represented by

$$\mathbf{n}^T\mathbf{u_b} = 0, \qquad (\mathbb{I} - \mathbf{n}\mathbf{n}^T)(\boldsymbol{\sigma}\cdot\mathbf{n}) = \mathbf{0}. \tag{Eq-7}$$

3. DISCRETIZATION AND GRADIENT RECONSTRUCTION

Now that we know the physics governing the system, we will use FV discretization to find the approximate solution of the problem in our domain.

3.1 Discretization Flow

The conservation equation is discretized using gauss law and stokes theorem to characterize flux on the interface.

$$\int_{V_i}\left(\frac{\partial(\phi\rho_\alpha s_\alpha)}{\partial t} - \nabla\cdot\left(\frac{\rho_\alpha k_{r\alpha}K}{\mu_\alpha}\nabla p\right)\right)dV = \int_{\partial V_i}\frac{\partial(\phi\rho_\alpha s_\alpha)}{\partial t}dV \mp \int_{\partial V_i}\frac{\rho_\alpha k_{r\alpha}q_\alpha}{\mu_\alpha}\,dS$$
$$\approx \frac{\Delta(\phi\rho_\alpha s_\alpha)_i}{\Delta t}V_i \mp \sum_{j\in\partial V_i}\delta_j\left(\frac{\rho_\alpha k_{r\alpha}}{\mu_\alpha}\right)_s q_{ij} = f_{\alpha i}V_i, \qquad \textbf{Eq-8}$$

where V_i is the volume of the discretized cell i, δ_j is the area of interface j which belongs to cell i. Δt is the time step size and $\Delta(\phi\rho_\alpha s_\alpha)_i$ is approximated by backward Euler in time i.e., $\Delta(\phi\rho_\alpha s_\alpha)_i = (\phi\rho_\alpha s_\alpha)_i^{n+1} - (\phi\rho_\alpha s_\alpha)_i^n$, subscript s denotes the property taken from the upwind direction. We also introduce a new term $q = -\mathbb{K}\boldsymbol{n}\cdot\nabla p$ we will call as the flux that is approximated in a nonlinear way.

3.2 Pressure Gradient Reconstruction

To get the approximation of flux we need to determine what value of ∇p between two cells across which flow is taking place. The starting point is to consider an interface between cells 1 and 2, we assume pressure is piecewise linear, pressure and flux are continuous across this interface j,

$$p_1 + (\boldsymbol{x}_j - \boldsymbol{x_1})^T\cdot\nabla p_1 = p_2 + (\boldsymbol{x}_j - \boldsymbol{x_2})^T\cdot\nabla p_2,$$
$$-\mathbb{K}_1\mathbf{n}_j\cdot\nabla p_1 = -\mathbb{K}_2\mathbf{n}_j\cdot\nabla p_2, \qquad \textbf{Eq-9}$$

p_1, p_2 are the pressures in the cells, $\boldsymbol{x_1}$, $\boldsymbol{x_2}$ are the cell centers and $\mathbb{K}_1, \mathbb{K}_2$ are the permeability tensors in the cells. The unit normal to the interface j is represented as $\mathbf{n}_j$. The continuity point $\boldsymbol{x}_j$ is chosen as the harmonic averaging point, which is detailed in [22].

Then using the information about harmonic averaging point we can derive the pressure gradient by using the equation,

$$\begin{bmatrix}(\boldsymbol{x}_{h2} - \boldsymbol{x_1})^T\\ (\boldsymbol{x}_{h3} - \boldsymbol{x_1})^T\\ (\boldsymbol{x}_{h4} - \boldsymbol{x_1})^T\end{bmatrix}\cdot\nabla p_1 = \begin{bmatrix}p_{h2} - p_1\\ p_{h3} - p_1\\ p_{h4} - p_1\end{bmatrix}, \qquad \textbf{Eq-10}$$

where $\boldsymbol{x}_{hi}$ is a known point in space, p_{hi} is our unknown pressure at that point which can be estimated by interpolating between cell 1 and cell i. The dimension of $\boldsymbol{x}_{hi} - \boldsymbol{x_1}$ is 3x3 matrix and right side of equation Eq-10 is a 3x1 vector. We choose the matrix and cell i such that coefficients in front of pressure from flux equation are non-negative. This is the criteria for an NTPFA approximation as weights cannot be negative when we combine the semi fluxes from both sides of the interface. But there can also be an instance where a perfect positive basis including the two-point cell i.e., cell 2 in this case, does not exist. So, we use a homogenization function suggested in [12], that allows us to interpolate pressure gradient by using cells which are not considered as immediate neighbors to our primary cell 1. We introduce (vector) homogenization function as:

$$\mathcal{H}^{\Sigma}_{1,k+1}(\boldsymbol{x} - \boldsymbol{x_1}) = \prod_{i=1}^{k}\left[\mathbb{I} + \frac{1}{\lambda^i_{i+1}}[\mathbb{K}_i - \mathbb{K}_{i+1\mathbb{I}}]\boldsymbol{n}_i\boldsymbol{n}_i^T\right](\boldsymbol{x} - \boldsymbol{x_1})$$
$$-\sum_{j=1}^{k}\left(\prod_{i=1}^{j-1}\left[\mathbb{I} + \frac{1}{\lambda^i_{i+1}}[\mathbb{K}_i - \mathbb{K}_{i+1\mathbb{I}}]\boldsymbol{n}_i\boldsymbol{n}_i^T\right]\right)\frac{r_1^j}{\lambda^j_{j+1}}(\mathbb{K}_j - \mathbb{K}_{j+1})\boldsymbol{n}_j, \qquad \textbf{Eq-11}$$

where $\Sigma = \{\delta_1, \delta_2, \dots, \delta_k\}$ denotes the set of interfaces and $\Theta = \{V_1, V_2, \dots, V_{k+1}\}$ is the set of cells through which we are homogenizing, $\lambda^i_{i+1} = \mathbf{n}_i^T\mathbb{K}_{i+1}\mathbf{n}_i$ and r_1^j is the shortest distance between collocation point in V_1 i.e. $\boldsymbol{x_1}$, interface j and the level of homogenization is represented by k. After we obtain the homogenization function, we can define our auxiliary conditions which will help us to reconstruct the pressure gradient, if we do not find a positive basis from the immediate neighbors of current cell-interface pair

$$\mathcal{H}^{\Sigma}_{1,i}(\boldsymbol{x_i} - \boldsymbol{x_1})\nabla p_1 = p_i - p_1. \qquad \textbf{Eq-12}$$

3.3 Nonlinear Flux for Flow

We will derive the formulation only for an internal interface in this paper. Information about boundary faces can be found in the thesis work [23]

$$q_1^{\delta} = c_{11}(p_1 - p_2) + c_{12}(p_1 - p_3) + c_{13}(p_1 - p_{G_1}), \qquad \textbf{Eq-13}$$

$$q_2^{\delta} = c_{21}(p_1 - p_2) + c_{22}(p_4 - p_2) + c_{23}(g_D - p_2). \quad \textbf{Eq-14}$$

here we are evaluating flux across interface δ, p_{G_1} and g_D correspond to pressures when we take Neumann or Dirichlet conditions respectively. The value of c_{ij} is always non-negative in this equation. We can combine both semi fluxes using the formula

$$q^{\delta} = \mu_1 q_1^{\sigma} + \mu_2 q_2^{\sigma}, \quad \textbf{Eq-15}$$

where μ_1 and μ_2 are weighting parameters and that lie between 0 and 1. They are chosen such that $\mu_1 + \mu_2 = 1$ and the flux will only remain with two-point pressures in the final form:

$$q^{\delta} = \mathbb{T}_1 p_1 - \mathbb{T}_2 p_2. \quad \textbf{Eq-16}$$

In equation Eq-16, $\mathbb{T}_1$ and $\mathbb{T}_2$ are non-negative and function of p_3, p_4, p_{G_1}, g_D, hence they will change according to how the pressure in the reservoir domain changes as p_3, p_4, p_{G_1}, g_D are unknowns in our formulation and we have to provide the values from previous iteration.

We also couple the discretization with fractures as considered in [24].

3.4 Discretization Mechanics

In this section, we derive nonlinear traction approximation for mechanics. The discretization framework will follow a similar path to NTPFA. First the discrete equation can be formulated by using stokes theorem as follows:

$$-\int_V \nabla \cdot \mathbb{C} : \frac{\nabla \boldsymbol{u} + \nabla \boldsymbol{u}^T}{2} \boldsymbol{d}V = -\sum_{\delta \in F(V)} \int_{\delta} \mathbb{C} : \frac{\nabla \boldsymbol{u} + \nabla \boldsymbol{u}^T}{2} \boldsymbol{n} dS \approx -\sum_{\delta \in F(V)} |\delta| \left[\mathbb{C} : \frac{\nabla \boldsymbol{u} + \nabla \boldsymbol{u}^T}{2} \right]_{\delta} \boldsymbol{n}_{\delta} = \mathbf{f}\,|V|, \quad \textbf{Eq-17}$$

where $|V|$ is the volume of our cell, $|\delta|$ is the area and $\boldsymbol{n}_{\delta}$ is the normal of interface δ which belongs to the current control volume V. Below we use the traction vector defined as $\boldsymbol{F} = -\left[\mathbb{C} : \frac{\nabla \boldsymbol{u} + \nabla \boldsymbol{u}^T}{2}\right]_{\delta} \boldsymbol{n}_{\delta}$ at the interface δ.

3.5 Displacement Gradient Reconstruction

First, we need to establish traction and displacement continuity on our interface with displacement being piecewise linear. The formulation of traction vector is taken from [17], where the 6x6 matrix $\mathbb{C}$ is split into six 3x3 submatrices $\mathbb{A}_i$.

$$\boldsymbol{F} = -\begin{bmatrix} \mathbf{n}^T\mathbb{A}_1 & \mathbf{n}^T\mathbb{A}_6^T & \mathbf{n}^T\mathbb{A}_5^T \\ \mathbf{n}^T\mathbb{A}_6 & \mathbf{n}^T\mathbb{A}_2 & \mathbf{n}^T\mathbb{A}_4^T \\ \mathbf{n}^T\mathbb{A}_5 & \mathbf{n}^T\mathbb{A}_4 & \mathbf{n}^T\mathbb{A}_3 \end{bmatrix} \begin{bmatrix} \nabla u \\ \nabla v \\ \nabla w \end{bmatrix}. \quad \textbf{Eq-18}$$

Then we can write the continuity of traction and displacement vectors as:

$$\boldsymbol{F} = -\begin{bmatrix} \mathbf{n}^T\mathbb{A}_1.\nabla u_1 + \mathbf{n}^T\mathbb{A}_6^T.\nabla v_1 + \mathbf{n}^T\mathbb{A}_5^T.\nabla w_1 \\ \mathbf{n}^T\mathbb{A}_6.\nabla u_1 + \mathbf{n}^T\mathbb{A}_2.\nabla v_1 + \mathbf{n}^T\mathbb{A}_4^T.\nabla w_1 \\ \mathbf{n}^T\mathbb{A}_5.\nabla u_1 + \mathbf{n}^T\mathbb{A}_4.\nabla v_1 + \mathbf{n}^T\mathbb{A}_3.\nabla w_1 \end{bmatrix} = -\begin{bmatrix} \mathbf{n}^T\mathbb{B}_1.\nabla u_2 + \mathbf{n}^T\mathbb{B}_6^T.\nabla v_2 + \mathbf{n}^T\mathbb{B}_5^T.\nabla w_2 \\ \mathbf{n}^T\mathbb{B}_6.\nabla u_2 + \mathbf{n}^T\mathbb{B}_2.\nabla v_2 + \mathbf{n}^T\mathbb{B}_4^T.\nabla w_2 \\ \mathbf{n}^T\mathbb{B}_5.\nabla u_2 + \mathbf{n}^T\mathbb{B}_4.\nabla v_2 + \mathbf{n}^T\mathbb{B}_3.\nabla w_2 \end{bmatrix}, \quad \textbf{Eq-19}$$

$$\boldsymbol{u}_1 + \boldsymbol{G}_1(\boldsymbol{x} - \boldsymbol{x}_1) = \boldsymbol{u}_2 + \boldsymbol{G}_2(\boldsymbol{x} - \boldsymbol{x}_2).$$

The values of $\boldsymbol{u}_i$ and $\boldsymbol{G}_i$ are

$$\boldsymbol{u}_i = [u_i, v_i, w_i], \quad \boldsymbol{G}_i = \begin{bmatrix} \frac{\partial u_i}{\partial x} & \frac{\partial u_i}{\partial y} & \frac{\partial u_i}{\partial z} \\ \frac{\partial v_i}{\partial x} & \frac{\partial v_i}{\partial y} & \frac{\partial v_i}{\partial z} \\ \frac{\partial w_i}{\partial x} & \frac{\partial w_i}{\partial y} & \frac{\partial w_i}{\partial z} \end{bmatrix},$$

Then traction can be characterized by splitting the harmonic part (corresponding to two-point cells) and transversal part (with transversal displacement gradient):

$$\boldsymbol{F} = -\boldsymbol{T}(\boldsymbol{u}_2 - \boldsymbol{u}_1) - \boldsymbol{\Gamma}\boldsymbol{G}_{\tau}, \quad \boldsymbol{T} = \boldsymbol{T}_1(r_1\boldsymbol{T}_2 + r_2\boldsymbol{T}_1)^{-1}\boldsymbol{T}_2, \quad \textbf{Eq-20}$$

where $\boldsymbol{T}$, $\boldsymbol{T}_1$ and $\boldsymbol{T}_2$ are 3x3 matrices, r_i is the distance from collocation point 1 to the interface between 1 and 2, $\boldsymbol{\Gamma}$ is the 3x9 coefficient matrix and transversal displacement gradient $\boldsymbol{G}_\tau$ is rearranged as 9x1 vector. The reconstruction process is carried on the transversal gradient and the equations look like:

$$\boldsymbol{\Gamma}\begin{bmatrix}\nabla u_1\\ \nabla v_1\\ \nabla w_1\end{bmatrix} = \boldsymbol{\Gamma}(\boldsymbol{Q})^{-1}\begin{bmatrix}\boldsymbol{u}_2-\boldsymbol{u}_1\\ \boldsymbol{u}_3-\boldsymbol{u}_1\\ \boldsymbol{u}_4-\boldsymbol{u}_1\end{bmatrix}, \qquad \textbf{Eq-21}$$

Here $(Q)^{-1}$ will be a 9x9 matrix and the product of $\Gamma(Q)^{-1}$ should yield a 3x9 matrix with all non-negative entries. This might be quite challenging, so we investigate the homogeneous problem where we can split the displacement gradients ∇u, ∇v, ∇w such that we only must invert 3x3 matrices. The auxiliary conditions are as follows:

$$\left(\left[\mathbb{I}\otimes(\boldsymbol{x}_2-\boldsymbol{x_1})^T\right]+r_2\,\boldsymbol{T}_2^{-1}\begin{bmatrix}\mathbf{n}^T(\mathbb{A}_1-\mathbb{B}_1) & \mathbf{n}^T(\mathbb{A}_6^T-\mathbb{B}_6^T) & \mathbf{n}^T(\mathbb{A}_5^T-\mathbb{B}_5^T)\\ \mathbf{n}^T(\mathbb{A}_6-\mathbb{B}_6) & \mathbf{n}^T(\mathbb{A}_2-\mathbb{B}_2) & \mathbf{n}^T(\mathbb{A}_4^T-\mathbb{B}_4^T)\\ \mathbf{n}^T(\mathbb{A}_5-\mathbb{B}_5) & \mathbf{n}^T(\mathbb{A}_4-\mathbb{B}_4) & \mathbf{n}^T(\mathbb{A}_3-\mathbb{B}_3)\end{bmatrix}\right)\begin{bmatrix}\nabla u_1\\ \nabla v_1\\ \nabla w_1\end{bmatrix} = \boldsymbol{u}_2-\boldsymbol{u}_1, \qquad \textbf{Eq-22}$$

which could be simplified in a homogeneous case where $\mathbb{A}_i = \mathbb{B}_i$. Again, the auxiliary conditions at boundaries will not be addressed in this description to keep it simple.

3.6 Nonlinear Traction for Mechanics

The traction can be represented as combination of harmonic part and weighted sum of transversal part of semi fluxes. The final form looks like:

$$\boldsymbol{F} = -\boldsymbol{T}(\boldsymbol{u}_2-\boldsymbol{u}_1)-\boldsymbol{\chi}_1\boldsymbol{F}_{\delta 1}-\boldsymbol{\chi}_2\boldsymbol{F}_{\delta 2}, \qquad \textbf{Eq-23}$$

with the weights that are represented by,

$$\boldsymbol{\chi}_1 = \begin{bmatrix}\mu_{x1} & 0 & 0\\ 0 & \mu_{y1} & 0\\ 0 & 0 & \mu_{z1}\end{bmatrix}, \qquad \boldsymbol{\chi}_2 = \begin{bmatrix}\mu_{x2} & 0 & 0\\ 0 & \mu_{y2} & 0\\ 0 & 0 & \mu_{z2}\end{bmatrix} \qquad \textbf{Eq-24}$$

where $\mu_{d1} + \mu_{d2} = 1 \quad \forall \quad d \in \{x,y,z\}\ i.e.\ \boldsymbol{\chi}_1+\boldsymbol{\chi}_2 = \mathbb{I}$,

both the transversal tractions can be calculated from,

$$\boldsymbol{F}_{\delta 1} = \boldsymbol{R}_2^c(\boldsymbol{u}_2-\boldsymbol{u}_1)+\boldsymbol{R}_3^c(\boldsymbol{u}_3-\boldsymbol{u}_1)+\boldsymbol{R}_4^c(\boldsymbol{u}_4-\boldsymbol{u}_1)+\boldsymbol{R}_5^c(\boldsymbol{r}_5-\alpha\boldsymbol{u}_1)+\boldsymbol{R}_6^c(\boldsymbol{r}_6-\alpha\boldsymbol{u}_1), \qquad \textbf{Eq-25}$$

$$\boldsymbol{F}_{\delta 2} = \boldsymbol{R}_1^d(\boldsymbol{u}_2-\boldsymbol{u}_1)+\boldsymbol{R}_7^d(\boldsymbol{u}_2-\boldsymbol{u}_7)+R_8^d(\boldsymbol{u}_2-\boldsymbol{u}_8)+\boldsymbol{R}_9^d(\alpha\boldsymbol{u}_2-\boldsymbol{r}_9)+\boldsymbol{R}_{10}^d(\alpha\boldsymbol{u}_2-\boldsymbol{r}_{10}). \qquad \textbf{Eq-26}$$

Once the terms corresponding to stencil other that two-point displacements are eliminated by our closure condition we will have traction as:

$$\boldsymbol{F} = \mathbb{T}_{\mathbb{1}}\boldsymbol{u}_1-\mathbb{T}_{\mathbb{2}}\boldsymbol{u}_2, \qquad \textbf{Eq-27}$$

where $\mathbb{T}_{\mathbb{1}}$ and $\mathbb{T}_{\mathbb{2}}$ are functions of $\boldsymbol{u}_3, \boldsymbol{u}_4, \boldsymbol{r}_5, \boldsymbol{r}_6, \boldsymbol{u}_7, \boldsymbol{u}_8, \boldsymbol{r}_9$ and $\boldsymbol{r}_{10}$. Also note that $\mathbb{T}_{\mathbb{1}}$ and $\mathbb{T}_{\mathbb{2}}$ are 3x3 matrices with non-negative entries.

4. SOLUTION STRATEGY

For both flow and mechanics, we use newton iterations and derive the Jacobian terms to solve the equation in the form:

$$\mathbb{A}\,\boldsymbol{u} = \boldsymbol{g}, \qquad \textbf{Eq-28}$$

with the $\mathbb{A}$ matrix assembled by using the flux information from equations Eq-16 and Eq-27. $\mathbb{T}_{\mathbb{1}}$ and $\mathbb{T}_{\mathbb{2}}$ will be 3x3 matrices for mechanics which means the $\mathbb{A}$ will be $3\boldsymbol{n}_c$ x $3\boldsymbol{n}_c$ matrix where $\boldsymbol{n}_c$ is the total number of control volumes.

$$\mathbb{A} = \begin{pmatrix}\mathbb{T}_{\mathbb{1}} & -\mathbb{T}_{\mathbb{2}}\\ -\mathbb{T}_{\mathbb{1}} & \mathbb{T}_{\mathbb{2}}\end{pmatrix}. \qquad \textbf{Eq-29}$$

Then we compute the residual vector and assemble our Jacobian matrix that comprises of derivatives of residual. So, it is better to evaluate the derivatives of $\boldsymbol{F}$ from Eq-27 with respect to each displacement in the nonlinear stencil and assemble our Jacobian.

$$\mathcal{J}_k \, \Delta x_k = -\mathcal{R}_k, \qquad \Delta x_k = x_{k+1} - x_k, \qquad \mathcal{J}_k = {}^{\partial \mathcal{R}_k}/_{\partial x_k} \qquad \textbf{Eq-30}$$

In Eq-30, $\mathcal{J}_k$ is evaluated by taking derivative of each element of $\mathcal{R}_k$ with x_k and $\mathcal{R}_k$ is a function of x_k. Also x_k is the unknown vector i.e., pressure or displacement in our case.

5. NUMERICAL EXPERIMENTS

In this section we will demonstrate how the scheme works in both flow and mechanics, then compare it with other types of discretization schemes. We use GMSH to generate our meshes for these example problems.

5.1 Multi-Phase Flow Problem

The goal of this experiment is to demonstrate multiphase flow when a heterogeneous permeability tensor is present in the domain. This is taken from [22]. Both structured and unstructured meshes are tested as shown in Table 1

Table 1: Multi-phase flow test for different meshes.

Mesh Type	*No. of cells*	*NI*	*NI/dt*
Coarse Transfinite	576	176	2.93
Coarse Hexahedrons	669	195	3.25
Adaptive Hexahedrons	3277	220	3.67
Adaptive Wedges	6702	244	4.07
Fine Transfinite	6561	248	4.13
Fine Wedges	7064	249	4.15

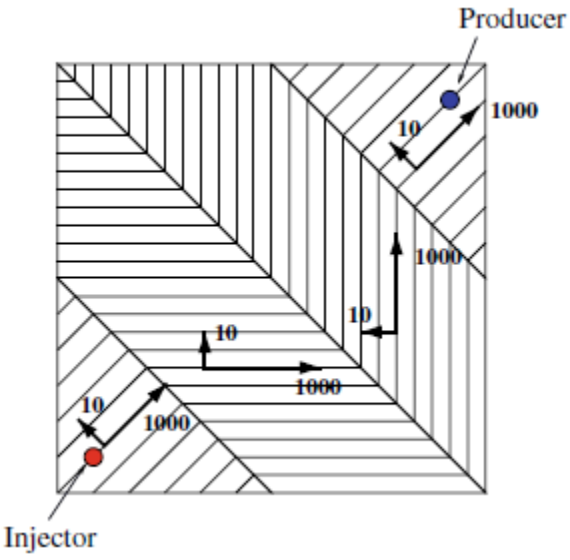

Figure 01: Problem setup of heterogeneous tensor taken from [22].

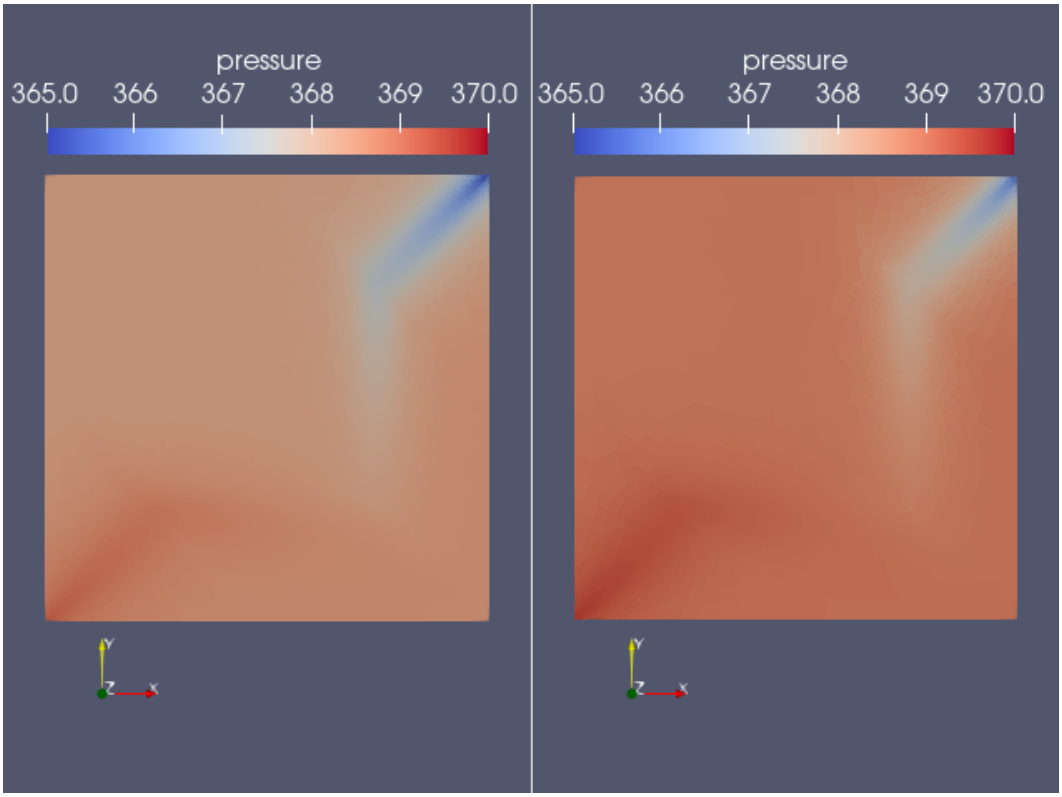

Figure 2: Pressure solution for unstructured adaptive wedges (left) and adaptive hexahedrons (right).

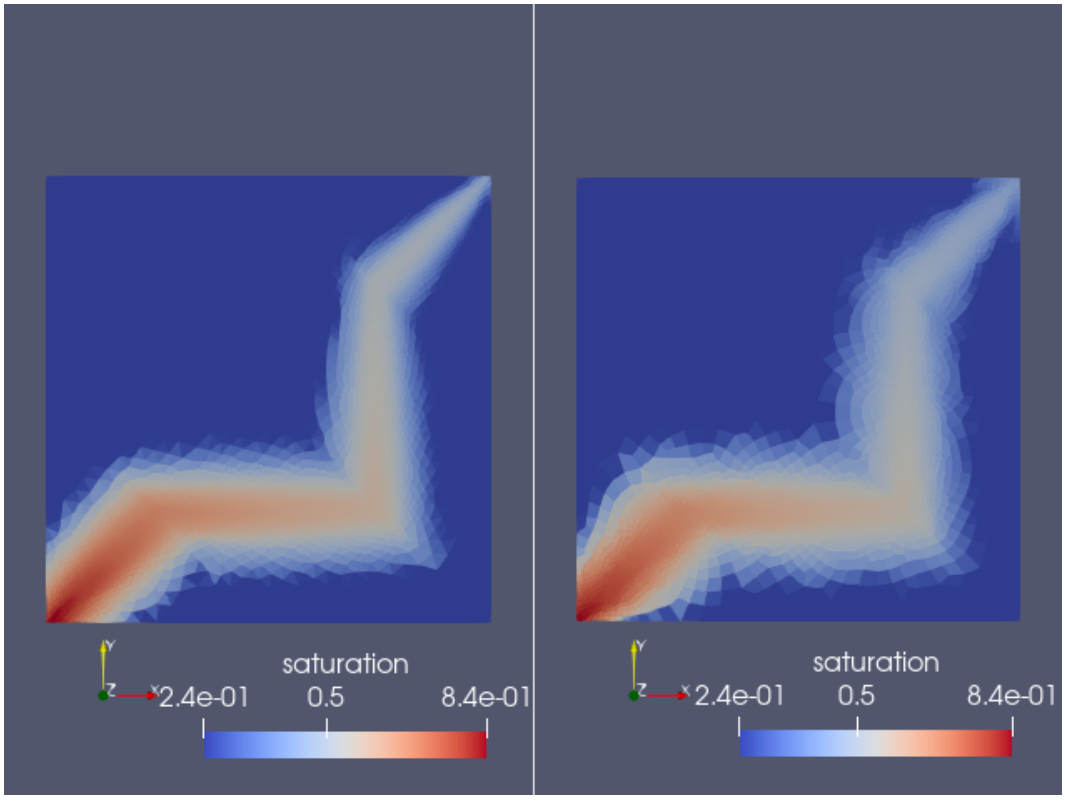

Figure 3: Saturation solution for unstructured adaptive wedges (left) and adaptive hexahedrons (right).

We can see from Figures 2, 3 the saturation front follows the direction of permeability tensor unlike the TPFA approximation [22], where the solution is dispersed.

5.2 Discrete Fracture Network

In this section, we try to test our discretizer when combined with the fracture network. We say fracture network, but the examples mainly consider flow in subsurface domain with matrix anisotropy and the set of single fracture and intersecting fractures. The flow will be driven by wells (we use the Peaceman well model). The following scenarios are considered:

Table 2: DFN + NTPFA.

Case	*Permeability (mD)*	*Well location*	*Aperture (mm)*	*t (days)*	*NI*	*NI/dt*
Single Fracture	$\mathbb{R}_{-45}\begin{bmatrix}500 & 0 & 0\\ 0 & 10 & 0\\ 0 & 0 & 10\end{bmatrix}\mathbb{R}_{-45}^{T}$	I (0,0) P (50, 100) P (100, 0)	1	300	136	4.5
Intersecting Fractures	$\mathbb{R}_{-5}\begin{bmatrix}1000 & 0 & 0\\ 0 & 10 & 0\\ 0 & 0 & 10\end{bmatrix}\mathbb{R}_{-5}^{T}$	I (0,0) P (50, 100) P (100, 50)	1	300	147	4.8

Where $\mathbb{R}_{-5}$ and $\mathbb{R}_{-45}$ are rotation matrices used in the z-axis. I and P, are locations of injectors and producers respectively and our domain spans $[0, 100]^2$. Total number of cells in both meshes are 2500.

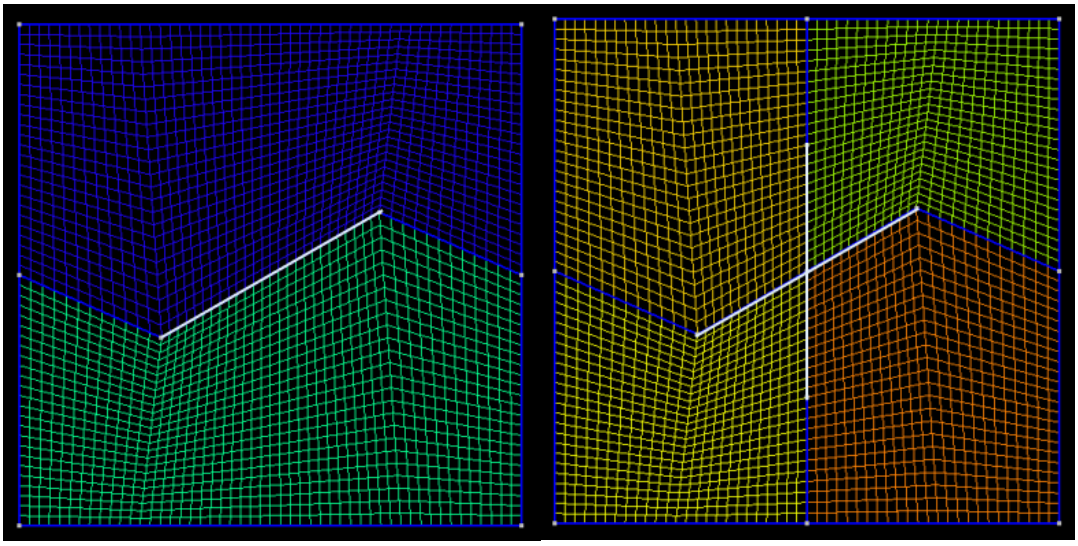

Figure 4: Meshes used for DFN+NTPFA with single fracture (left) and intersecting fractures (right).

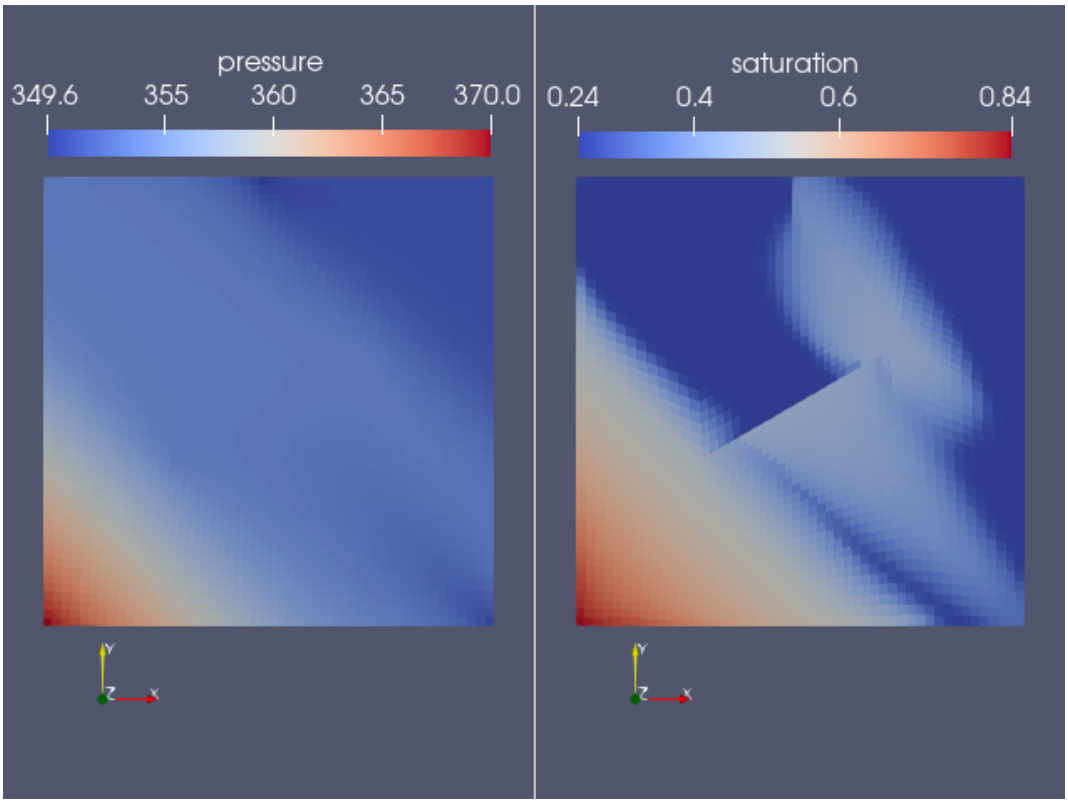

Figure 5: Solution of DFN+NTPFA with single fracture, pressure (left) and saturation (right).

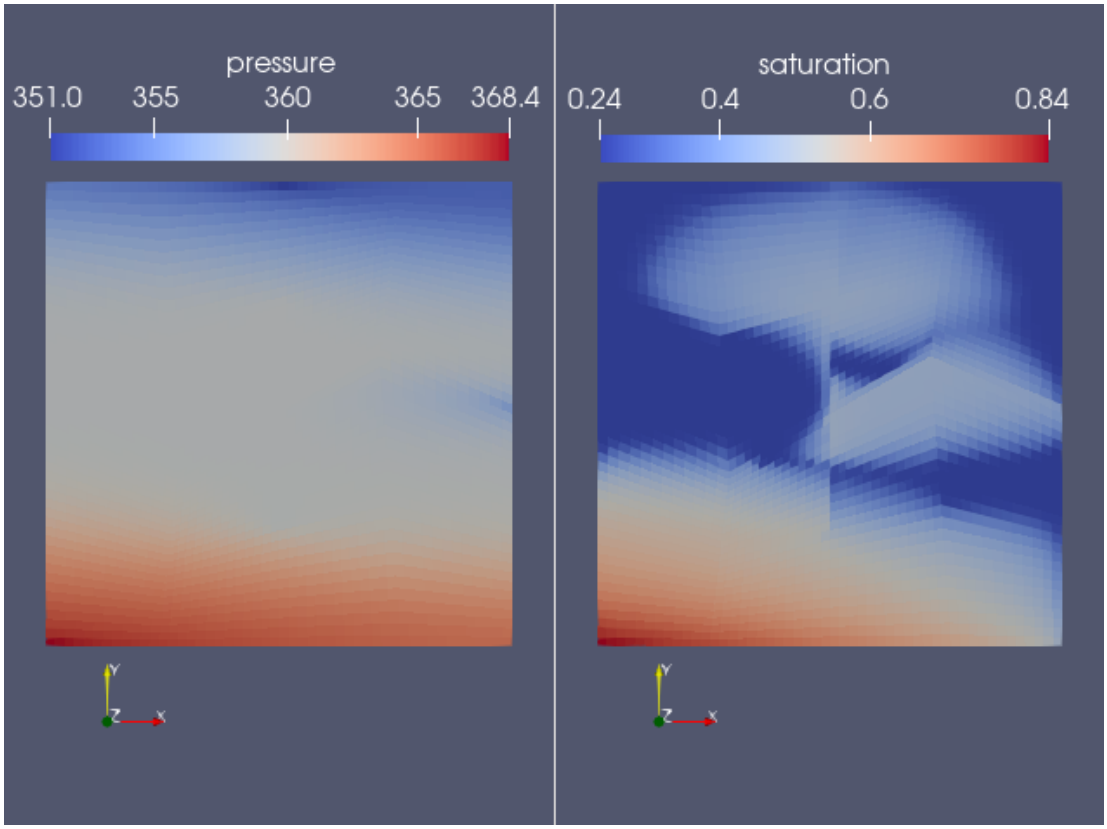

Figure 6: Solution of DFN+NTPFA with intersecting fracture, pressure (left) and saturation (right).

As we use a non-K-orthogonal grid, we see primary direction of flow is corresponding to the permeability tensor, then due to the presence of fracture the flow is deviated.

5.3 Compression and Shear (Mechanics)

In this part, we take the following problem previously discussed in [21]. For pure mechanics, as we are not considering any fracture formation and slip along the fracture, we will analyze the traction profile on a specific line or feature in our grid domain. The setup of the problem is formulated in Figure 7.

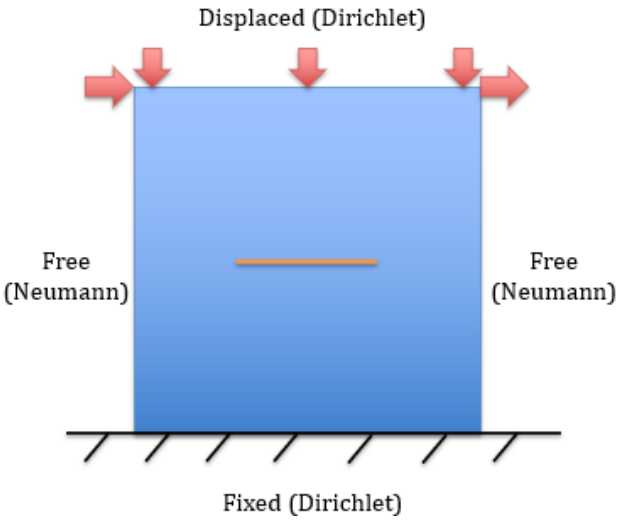

Figure 7: Problem setup on 3D extruded grid, roller boundary conditions in the z+ and z- planes.

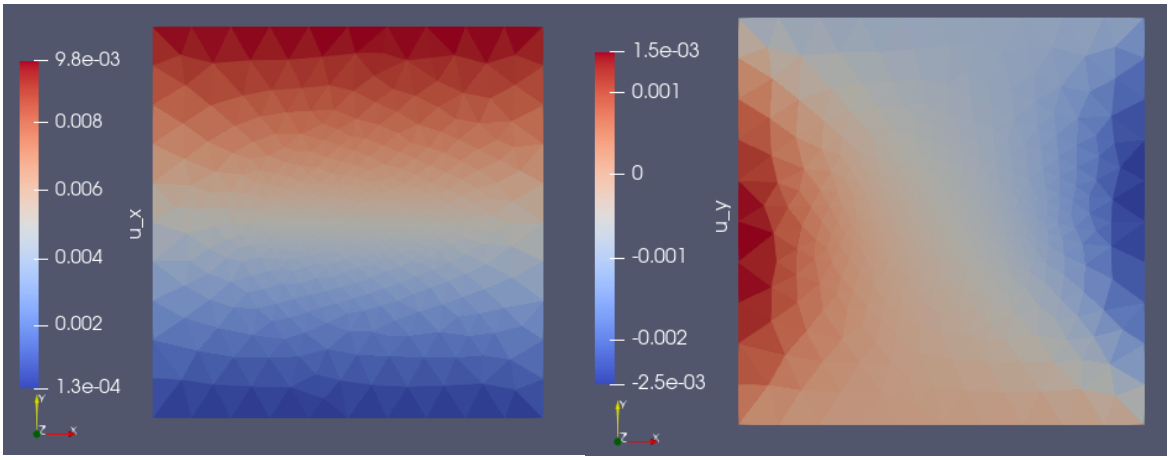

Figure 8: Deformation in our domain u_x (left) and u_y (right).

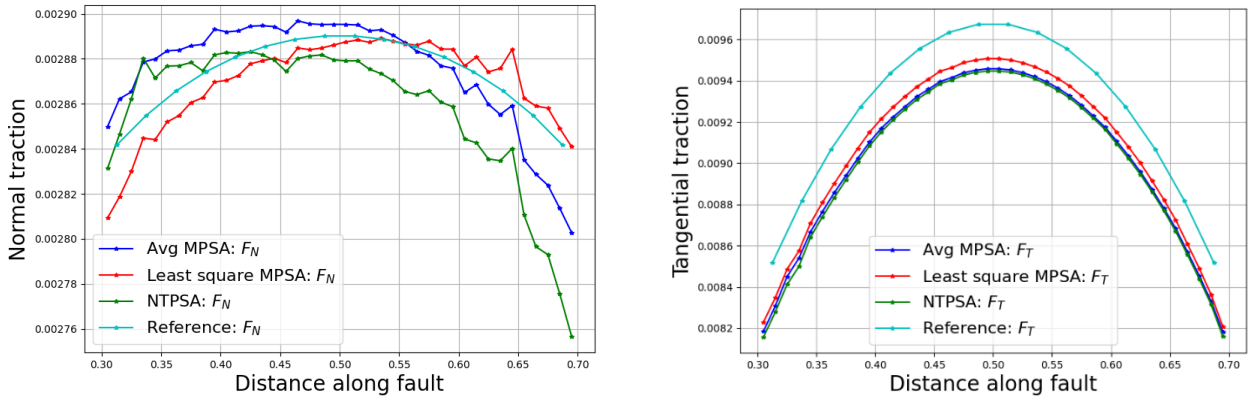

Figure 9: Traction along the orange plane with F_n (left) and F_t (right).

First, we must perform domain shifting such that our initial conditions u, v and w are from 10, 10 and 0 respectively for the NTPSA to have non-negative weights. We present solutions from coarse wedges as there are some oscillations observed when implementing on unstructured wedges. From the solutions in Figures~8 and 9, we see some oscillations in normal traction along the orange plane described in Figure 7. We also compare this result with MPSA approximation form [17] and both these methods present oscillations. A more detailed analysis on oscillations will be added in the future work.

6. CONCLUSION

Nonlinear discretization methods in subsurface flow simulation are known for their robustness by not only approximating an accurate form of flux (taking anisotropy and heterogeneity) across the interface, but also giving a monotone solution with no oscillations which are usually observed in MPFA. The flux approximation specifically developed in this project can reconstruct the pressure gradient in most distorted meshes with severe anisotropy by using the homogenization technique, which helps us to find a positive basis considering the minimum number of cells in the process.

The insights gained from NTPSA formulation can be used to formulate a Nonlinear poromechanical discretization framework in FV domain. When we investigate any practical applications such as high enthalpy geothermal simulations, coupling both flow and mechanics is important to understand how deformation looks during the process. By coupling them in a nonlinear FV framework we can make sure oscillations in primary variable are reduced.

REFERENCES

[1] K. Aziz, A. Settari. Petroleum Reservoir Simulation, Applied Science Publishers LTD, 1979.

[2] I. Aavatsmark, "Discretization on Non-Orthogonal, Quadrilateral Grids for Inhomogeneous, Anisotropic Media," *Journal of Computational Physics,* vol. 127, no. 1, pp. 2-14, 1996.

[3] Edwards Michael G., Rogers Clive F., "Finite volume discretization with imposed flux continuity for the general tensor pressure equation," *Computational Geosciences,* vol. 2, pp. 259-290, 1998.

[4] I. Aavatsmark, "An introduction to multipoint flux approximations for quadrilateral grids," *Computational Geosciences,* vol. 6, pp. 405-432, 2002.

[5] I. Aavatsmark and G. T. Eigestad and B. T. Mallison and J. M. Nordbotten, "A Compact Multipoint Flux Approximation Method with Improved Robustness," *Numerical Methods for Partial Differential Equations,* pp. 1329-1360, 2008.

[6] D. S. Kershaw, "Differencing of the diffusion equation in Lagrangian hydrodynamic codes," *Journal of Computational Physics,* vol. 39, no. 2, pp. 375-395, 1981.

[7] C. L. Potier, "Schéma volumes finis monotone pour des opérateurs de diffusion fortement anisotropes sur des maillages de triangles non structurés," *Comptes Rendus Mathematique,* vol. 341, no. 12, pp. 787-792, 2005.

[8] E. Bertolazzi and G. Manzini, "A CELL-CENTERED SECOND-ORDER ACCURATE FINITE VOLUME METHOD FOR CONVECTION–DIFFUSION PROBLEMS ON UNSTRUCTURED MESHES," *Mathematical Models and Methods in Applied Sciences,* vol. 14, pp. 1235-1260, 2004.

[9] K. Nikitin, K. Terekhov, Y. Vassilevski, "A monotone nonlinear finite volume method for diffusion equations and multiphase flows," *Computational Geosciences,* vol. 18, pp. 311-324, 2013.

[10] A. A. Danilov and Y. V. Vassilevski, "A monotone nonlinear finite volume method for diffusion equations on conformal polyhedral meshes," vol. 24, pp. 207-227, 2009.

[11] K. Lipnikov and D. Svyatskiy and Y. Vassilevski, "Interpolation-free monotone finite volume method for diffusion equations on polygonal meshes," *Journal of Computational Physics,* vol. 228, pp. 703-716, 2009.

[12] K. Terekhov, B. Mallison, H. Tchelepi, "Cell-centered nonlinear finite-volume methods for the heterogeneous anisotropic diffusion problem," *Journal of Computational Physics,* vol. 330, 2016.

[13] Z-M. Gao, J. Wu, "A Second-Order Positivity-Preserving Finite Volume Scheme for Diffusion Equations on General Meshes," *SIAM Journal on Scientific Computing,* vol. 37, pp. 420-438, 2015.

[14] M. Schneider, B. Flemisch, R. Helmig, K. Terekhov, H. Tchelepi, "Monotone nonlinear finite-volume method for challenging grids," *Computational Geosciences,* vol. 22, 2018.

[15] Tuković, Z. and Ivanković, A. and Karač, A., "Finite-volume stress analysis in multi-material linear elastic body," *International Journal for Numerical Methods in Engineering,* vol. 93, pp. 400-419, 2013.

[16] N. J. Martin, "Cell-centered finite volume discretizations for deformable porous media," *International Journal for Numerical Methods in Engineering,* vol. 100, pp. 399-418, 2014.

[17] K. M. Terekhov and H. A. Tchelepi, "Cell-centered finite-volume method for elastic deformation of heterogeneous media with full-tensor properties," *Journal of Computational and Applied Mathematics,* vol. 364, 2020.

[18] E. Keilegavlen, J.M. Nordbotten, "Finite volume methods for elasticity with weak symmetry," *International Journal for Numerical Methods in Engineering,* vol. 112, pp. 939-962, 2017.

[19] D. Voskov, "Operator-based linearization approach for modeling of multiphase multi-component flow in porous media," *Journal of Computational Physics,* vol. 337, 2017.

[20] Y. Wang, D. Voskov, D. Bruhn, "An efficient numerical simulator for geothermal simulation: A benchmark study," *Applied Energy,* vol. 264, 2020.

[21] A. Novikov and D.V. Voskov and M. Khait and H. Hajibeygi and J.D. Jansen, "A Collocated Finite Volume Scheme for High-Performance Simulation of Induced Seismicity in Geo-Energy Applications," *SPE,* no. SPE 203903-MS, 2021.

[22] Y. Vassilevski, K. Terekhov, K. Nikitin, I. Kapyrin, Parallel Finite Volume Computation on General Meshes, 2020.

[23] S. R. T. Tripuraneni, D. Voskov and A. Novikov, "Non-Linear Finite Volume discretization for Subsurface Flow and Mechanics problem," Delft University of Technology master thesis, 2021.

[24] Karimi-Fard, M. and Durlofsky, L.J. and Aziz, K., "An Efficient Discrete Fracture Model Applicable for General Purpose Reservoir Simulators," 2003.